Glass vs. Crystal: a Balancing Act between Competing Intermolecular Interactions

Audrey Laventure,† Thierry Maris,† Christian Pellerin† and Olivier Lebel*,‡

† Département de chimie, Université de Montréal, Montréal, QC, H3C 3J7, Canada.

‡ Department of Chemistry and Chemical Engineering, Royal Military College of Canada, Kingston, ON, K7K 7B4, Canada.

ABSTRACT: Hydrogen (H) bonds can be used either for crystal engineering or for designing compounds capable of forming very stable glassy phases. Herein, a second type of directional non-covalent interaction, π-π stacking, is introduced to establish the interplay between both types of interactions on crystal and glass formation. For this purpose, two mexylaminotriazine derivatives incorporating 2,3,4,5,6-pentafluorostilbene groups (with or without a H-bond donor at the 2 position of the triazine) and their non-fluorinated analogues were synthesized to compare their glass-forming and crystallization properties. While all four compounds showed glass-forming ability, only the fluorinated compounds showed crystallization with kinetics strongly affected by the presence or absence of the H-bond donor group. X-ray diffraction of the pentafluorostilbene-containing derivatives revealed an extended π-π stacking interaction, different from that of 2,3,4,5,6-pentafluorostilbene. These results, combined with infrared spectroscopy measurements, suggest that π-π stacking promotes crystallization, while hydrogen bonding impedes it, due to the higher conformational constraints imposed by π-π stacking, thereby decreasing the degrees of liberty and the possibilities for secondary interactions with other molecules.

Introduction

Molecular glasses, or molecular amorphous materials, are small organic molecules that can readily form glassy phases and remain indefinitely amorphous under ambient conditions.[1-7] While these properties are shared with inorganic glasses (e.g. SiO_2) and polymers, molecular glasses are unique among amorphous materials because their discrete, monodisperse chemical structures provide several advantages such as an easier purification and characterization, more reproducible processing conditions, and more homogeneous behavior between different samples and within the same sample. While there are disadvantages associated with small molecules, including lower yield stress and mechanical resistance, their principal limitation is their propensity to crystallize over time, as the glassy state is metastable.[1-3]

Just as structural guidelines have been identified to promote and influence the crystallization of organic compounds, certain structural elements are known to combat crystallization, both in terms of their effects on the propensity to form glasses under mild processing conditions (glass-forming ability, GFA) and on the kinetic resistance to crystallization (glass stability, GS). Irregular molecular shapes, non-planarity, the presence of flexible groups, and conformational ambiguity have emerged as structural features that promote glass formation, as opposed to crystallization.[4-6, 8-9] The design of molecular glasses with improved resistance to crystallization has led to their use in a wide range of practical applications, ranging from photonics,[10-12] opto-electronics[4-6] and nanolithography,[13-14] to formulations for amorphous drugs.[15-16]

Although strong and directional intermolecular interactions have long been associated with crystallization and are a well-known tool for engineering crystals, the presence of hydrogen (H) bonds does not necessarily prevent compounds from forming glasses, as evidenced by mexylaminotriazine derivatives.[17-20] This class of compounds has demonstrated strong GFA, often remaining completely amorphous under cooling from the melt at rates as low as 0.05 °C/min, and high to extreme GS, even at temperatures above their glass transition temperature (T_g), depending on the triazine substituents. It was recently shown that the principal factor contributing to glass formation is the presence of conformers of similar energy with high interconversion barriers, thereby resulting in similar populations of different conformers and to suboptimal packing.[21-22] Nevertheless, the presence of hydrogen bonds substantially increases the T_g of molecular glasses compared to analogous compounds that cannot H-bond, therefore limiting molecular mobility and contributing to higher glass stability in the vitreous state. Furthermore, H-bonds remain present in the material even at temperatures well above T_g, though the degree of H-bonding decreases with temperature, thus providing molecular cohesion in the viscous state that contributes to a high glass-forming ability.[22-23]

It is currently not known if other types of non-covalent interactions can provide a similar GFA and GS behavior in molecular glasses. Moreover, when two different types of

such interactions are present, the outcome of their interplay is unclear: it may enhance glass formation by increasing the probability of kinetic trapping in multiple conformational and aggregation states that prevent efficient regular packing, or it may promote crystallization if the additional interaction rather favors the adoption of a specific conformation and/or local-scale packing that is closer to the equilibrium state in the energy landscape.

The present study therefore aims to study the effect of the simultaneous presence of two orthogonal strong intermolecular interactions on glass formation in mexylaminotriazine derivatives. Among available non-covalent interactions, electrostatic interactions often interfere with hydrogen bonds, while the long alkyl chains associated with van der Waals interactions may result in T_g values that are under ambient temperature, thereby limiting their usefulness for most practical applications.[18] On the other hand, donor-acceptor aromatic interactions, commonly referred to as π-π stacking,[24] is a type of non-covalent interaction that is widely studied[25] because of its implication in various domains ranging from supramolecular chemistry to chemical biology (e.g. DNA and protein tertiary structures).[26-27] Its interplay with hydrogen bonding is still explored, but the combination of both interactions has been successfully exploited to design specific supramolecular structures, such as synthetic molecular strands,[28] in addition to being revealed as an efficient strategy to enhance the performances of solar cells[29] and to prepare luminescence-switching solids.[30] Aromatic moieties capable of π-π stacking can be easily introduced as substituents on the mexylaminotriazine core. As it is a weaker interaction than hydrogen bonding, it is crucial to introduce groups that will enhance π-π stacking strength in order to study the effect of two competing intermolecular interactions on the crystallization/vitrification behavior of molecular compounds. For this purpose, the benzene-perfluorobenzene couple is a prime model since it is a well-known case of strong and directional π-π stacking which has been used as supramolecular synthons in crystal engineering.[31] The case of 2,3,4,5,6-pentafluorostilbene, where molecules stack in columns with alternating fluorinated and non-fluorinated groups is one example, among others, where this pattern is used.[32-33] It has been exploited notably to prepare supramolecular nanofibers and hydrogels,[34] and used in liquid crystals, polymeric materials,[35] and nonlinear optical amorphous molecular materials.[36-38]

Herein, two mexylaminotriazine derivatives incorporating a 2,3,4,5,6-pentafluorostilbene moiety, one with a H-bond donor as the headgroup (2 position of the triazine) and the other without, and their two non-fluorinated analogues, were synthesized and studied. The fluorinated derivatives proved capable of glass formation but they crystallized upon heating, while their non-fluorinated analogues remained in the glassy state indefinitely. X-ray diffraction of single crystals of the fluorinated derivatives revealed that, unlike 2,3,4,5,6-pentafluorostilbene, these molecules form extended π-π stacking interactions involving the stilbene moieties along with the triazine and mexyl rings. Infrared spectroscopy (IR) measurements showed that hydrogen bonding in the amorphous material impedes crystallization while the π-π stacking interactions instead favor crystallization. The outcome for the different derivatives is explained, on one hand, by the competition between the molecular disorder induced by multiple H-bonds that tend to kinetically trap in the glassy state the non-fluorinated compounds in multiple disordered conformations and, on the other hand, by the higher degree of conformational homogeneity and the local packing enabled by the π-π stacking of pentafluorostilbene derivatives that promotes their crystallization.

Results and Discussion

Synthesis

The most straightforward strategy to synthesize mexylaminotriazine derivatives incorporating stilbene groups involves reacting 2-methylamino-4-mexylamino-6-[(3-formylphenyl)amino]-1,3,5-triazine **1a**, which has already been reported in the literature,[19] and analogue **1b**, by a Wittig reaction with the corresponding benzyltriphenylphosphonium salts in the presence of NaH in DMF (Scheme 1).[39]

Target stilbenes **2a**-**b** and **3a**-**b** (also referred to subsequently as NHMe/Ph, NMe_2/Ph, NHMe/F_5Ph, and NMe_2/F_5Ph, respectively) were thusly accessed in one synthetic step and in 48-74 % yields after purification on silica. Whereas fluorinated analogues NHMe/F_5Ph and NMe_2/F_5Ph **3a**-**b** were obtained exclusively as the *E* isomer, owing to the electron-withdrawing character of the 2,3,4,5,6-pentafluorophenyl group, parent compounds NHMe/Ph and NMe_2/Ph **2a**-**b** were obtained as *E*/*Z* mixtures. Compound **2a** could only be enriched to a 3:1 *E*/*Z* ratio by flash chromatography because of the highly polar nature of the compound, whereas attempts to enrich the *E* isomer by chemical methods (I_2-mediated isomerization for example) resulted in the formation of undesirable side products. On the other hand, compound NMe_2/Ph **2b** gave a 1:1 mixture of isomers that could be partially separated by chromatography using hexanes/ethyl acetate 7:3 as eluent, thereby allowing to obtain a small sample of pure *E* isomer that could be studied.

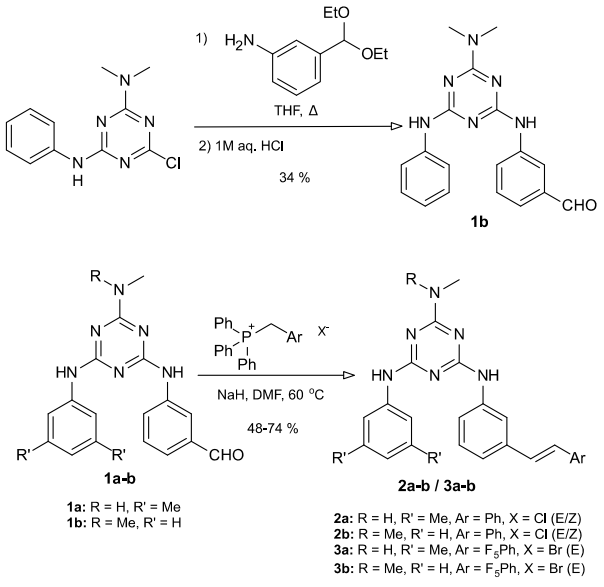

Scheme 1. Synthesis of compounds **2a**-**b** and **3a**-**b**.

Both precursors **1a**-**b** were used in order to better discriminate between the effects of the presence of the pentafluorophenyl group and hydrogen bonding on glass-forming ability. In compounds **1b**, **2b** and **3b**, the methylamino headgroup and mexylamino group, which are both known as being excellent at promoting glass formation, are replaced by dimethylamino and phenylamino groups, respectively, which were previously shown to give rise to mediocre GFA and poor GS.[18-19]

Thermal Properties

Differential scanning calorimetry (DSC) was used to evaluate the thermal properties of stilbene derivatives **2a**-**b** and their fluorinated analogues **3a**-**b**. Their glass transition temperature (T_g) values and their critical cooling rate (R_c), i.e. the slowest rate at which a compound can be cooled down from the melt without showing detectable crystallization signs by DSC, are listed in Table 1 (representative DSC scans are shown in Figure S1 of the Supporting Information). As expected, both stilbene derivatives bearing a H-bond donating methylamino headgroup, NHMe/Ph **2a** and NHMe/F_5Ph **3a**, readily form glasses even upon extremely slow cooling (R_c < 0.05 ºC/min). They are kinetically stable at ambient temperature and do not crystallize upon heating at a rate of 10 ºC/min. Surprisingly, both compounds show the same T_g at 78 ºC. The presence of a pentafluorophenyl ring in compound **3a** does not result in a higher T_g in spite of stronger aromatic interactions, which leads to the conclusion that the π-π interactions are not dominant over the H-bonding when this compound is in its amorphous state. The T_g of these two compounds is lower than that of the bis(mexylamino) parent compound (94 ºC) but similar to other closely similar triazine analogues.[19]

In contrast with compounds **2a**-**3a**, DSC measurements revealed fundamental differences in the thermal behavior of compounds NMe_2/Ph and NMe_2/F_5Ph **2b**-**3b**. Despite its headgroup and ancillary groups known to induce poor GFA, stilbene derivative NMe_2/Ph **2b** proved capable of forming glasses even when cooled as slow (R_c < 0.05 ºC/min) as its H-bonded analogue **2a**, with a lower T_g value of 50 ºC, and without signs of crystallization upon heating. Because the sample used contained only the *E* isomer, this lower T_g value compared to its NHMe/Ph **2a** counterpart cannot be attributed to a *E*/*Z* mixture, but rather mainly to the headgroup's lack of H-bond donating capability, which we have previously shown

Table 1. Glass transition temperature (T_g) and critical cooling rate (R_c) of compounds **2a-b** and **3a-b**.

Compound	Headgroup/Stilbene	T_g (ºC)	R_c (ºC/min)
2a	NHMe/Ph	78	< 0.05
2b	NMe_2/Ph	50	< 0.05
3a	NHMe/F_5Ph	78	< 0.05
3b	NMe_2/F_5Ph	67	10 < R_c < 50

to be the most influential group on thermal properties, and also to the presence of the phenyl ancillary groups expected to decrease the T_g of 20 ºC compared to mexyl groups.[19] On the other hand, the perfluorinated analogue NMe_2/F_5Ph **3b** only resists crystallization when cooled at rates higher than 10 ºC/min, more than 2 orders of magnitude faster than all other compounds, and undergoes cold crystallization above its T_g of 67 ºC. This T_g value is intermediate between those of the H-bonded compounds (78 ºC) and of its non-fluorinated analogue (50 ºC). It is lower than for **3a** because of the incapability of the headgroup to establish H-bonds and the less bulky ancillary group (phenyl instead of mexyl). It is however 17 °C higher than for **2b** because the presence of the perfluorophenyl moiety favors stronger aromatic interactions in comparison with the non-fluorinated one. Thus, both types of strong non-covalent interactions can contribute to increasing the T_g of molecular glasses when crystallization is avoided. The cold-crystallization behavior observed in the DSC heating scans of compound **3b** suggests that stronger aromatic interactions involving pentafluophenyl groups in the viscous sample favor crystallization at slow cooling rates. As it will be shown below, they impose a more rigid organization between molecules that promotes the regular packing found in crystals.

Hydrogen Bonding Changes upon Cooling from the Melt

To further investigate the respective influences of hydrogen bonding and aromatic interactions on glass-forming ability, variable-temperature infrared spectroscopy (IR) was used to study the four compounds in situ during their cooling process (2 ºC/min) from the melted state. Indeed, we have shown in a recent study that tracking the changes occurring in the mid-IR NH stretching region and applying chemometrics analysis provide quantitative insight on the evolution of H-bonding (average number of interactions and their enthalpy of formation) during the vitrification phenomenon.[22] Figure 1 displays the evolution with temperature of the "free" (3430-3400 cm^{-1}) and the "bonded" (3270-3280 cm^{-1}) NH stretching bands for the four compounds. Upon cooling from 200 ºC (red) down to 40 ºC (blue) compounds NHMe/Ph **2a** and NHMe/F_5Ph **3a** (Figure 1a and 1c), the absorbance of the "free" band decreases as the absorbance of the "bonded" band increases. This shows that the number of strong H-bonds increases as the compounds (initially in their viscous state) vitrify. This behavior is consistent with other mexylaminotriazine molecular glasses for which a larger average number of strong H-bonds was also found in the vitreous phase.[22] The average number of strongly bonded NH per molecule increases, when cooling from 200 to 40 ºC, from 1.2 to 2.1 for compound NHMe/Ph **2a** and from 1.4 to 2.3 for compound NHMe/F_5Ph **3a**. The values at T_g (78 ºC) are very similar for both compounds, 2.0 and 2.2, which is consistent with their identical T_g. These values are slightly lower than for the bis(mexylamino) parent compound (2.3 at its T_g of 94 °C) and thus in agreement with the trend we have previously demonstrated where T_g increases with the average

number of strongly bonded NH groups (headgroup and linkers) per molecule at T_g.[22]

In contrast with compounds with the NHMe headgroup, Figure 1b and 1d shows that the absorbance of both "free" and "bonded" bands increases for compounds NMe_2/Ph **2b** and NMe_2/F_5Ph **3b** upon cooling. The increase of the "free" band is slight for NMe_2/Ph **2b** but it is much more important in the case of the fluorinated compound **3b**, with the band becoming much narrower than for any other compound. Since its critical cooling rate is much higher than 2 ºC/min, it should be emphasized that this compound undergoes partial crystallization upon cooling, by opposition to vitrification for the other compounds (see DSC curves shown in Figure S1b). Moreover, the spectrum recorded at 200 ºC already shows evidences of crystallinity since its melting point is 202 ºC. Unfortunately, the shape of the "free" bands complicates the chemometrics analyses, making it difficult to evaluate with reliability the average number of bonded NH groups of these compounds.

However, it is clear that for compound **3b**, the absorbance of the "free" NH band is larger than the "bonded" one after cooling to 40 ºC. This relative proportion has not been observed previously in neither the vitreous nor the crystalline state of any analogous compounds. To confirm that the presence of this large fraction of "free" NH groups is characteristic of the crystalline state of compound NMe_2/F_5Ph **3b**, variable-temperature IR spectra were measured upon heating a completely amorphous sample (obtained by quenching melted **3b** much faster than its R_c using liquid nitrogen) since DSC heating scans show that it undergoes cold crystallization. Figure S2 in Supporting Information displays the series of spectra recorded from 40 ºC (blue) in the amorphous state up to 120 ºC (red) in the crystalline state. At 40 ºC, the "free" NH band is broad and, as temperature increases and the compound undergoes its glass transition, its absorbance starts to increase while that of the "bonded" NH band decreases, the expected behavior for an amorphous compound.

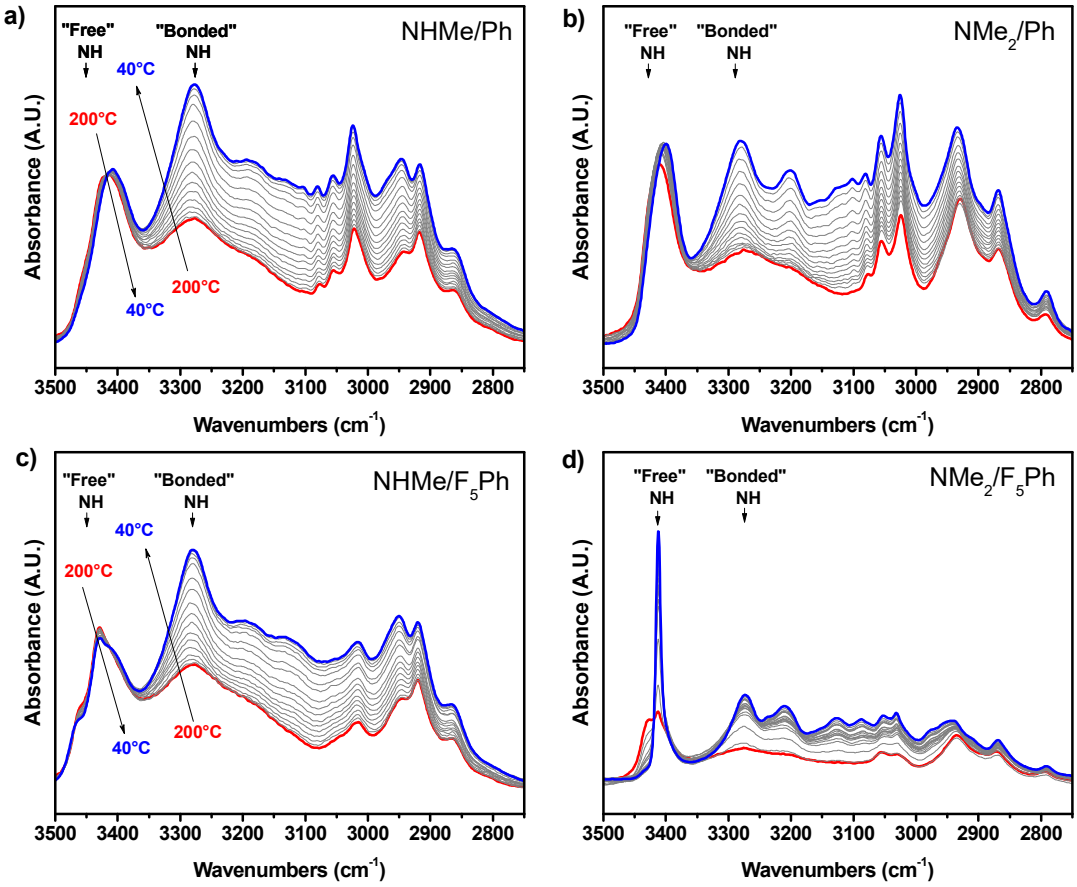

Figure 1. Variable-temperature IR spectra of compounds a) NHMe/Ph **2a**, b) NMe_2/Ph **2b**, c) NHMe/F_5Ph **3a** and d) NMe_2/F_5Ph **3b** recorded with a cooling rate of 2 °C/min.

The "free" NH band then becomes narrower during the cold crystallization process. The spectrum of the quenched sample at 40 °C is similar to those of the other compounds recorded in the vitreous state, indicating that the fraction of "bonded" NH groups is higher in the glassy sample, while the spectrum in the cold-crystallized state is qualitatively very similar to the spectrum at 40 °C in Figure 1d, which supports the fact that a larger amount of "free" NH are present in the crystalline state than in the glassy state. These observations imply that the crystallization of NMe_2/F_5Ph **3b** requires the disruption of at least some of the H-bonds present in the amorphous state and that it must therefore be accompanied by the formation of another interaction than H-bonding, shown in the next section to be the aromatic interaction involving the pentafluorophenyl group.

Crystal Structures of Compounds NHMe/F_5Ph 3a and NMe_2/F_5Ph 3b

While pentafluorostilbene derivative NMe_2/F_5Ph **3b** could be easily crystallized from DMSO/CH_2Cl_2, single crystals of NHMe/F_5Ph **3a** suitable for X-ray diffraction could be grown directly by thermal annealing at 150 ºC during 24 h even if it readily forms stable glasses. In contrast, all attempts to crystallize non-fluorinated analogues NHMe/Ph **2a** and NMe_2/Ph **2b** proved unsuccessful, instead yielding amorphous precipitates.

Compound NMe_2/F_5Ph **3b** crystallized in the triclinic P-1 space group, with two molecules per unit cell. Figure 2a shows that both arylamino substituents point towards different directions with all four aromatic rings roughly coplanar and with the stilbene moiety oriented towards the headgroup rather than away from the rest of the molecule, giving the molecule a more compact Z-like shape (additional views are provided in Figure S3). The pentafluorostyryl group of the stilbene moiety is disordered over two positions, though this does not change significantly the general shape of the molecules. This orientational disorder is caused by the pedal motion of the two benzyl

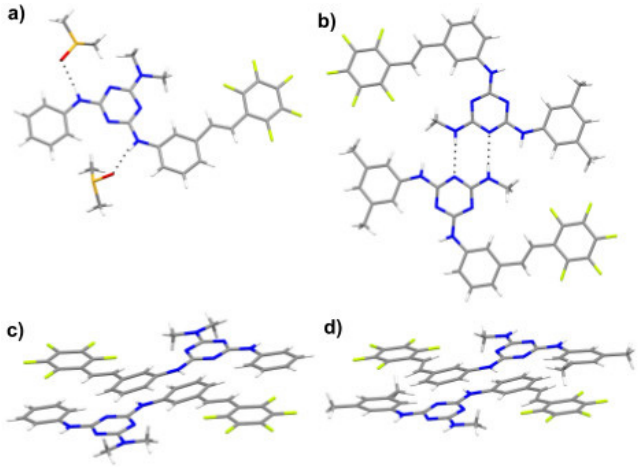

Figure 2. View of intermolecular interactions in the crystal structures of compounds NHMe/F_5Ph **3a** and NMe_2/F_5Ph **3b**. a) Hydrogen bonding with DMSO molecules of compound NMe_2/F_5Ph **3b**; b) hydrogen-bonded dimer of compound **3a**; c) π-stacked dimer of compound **3b**; d) π-stacked dimer of compound **3a**. Only one of two disordered positions for the stilbene group of compound **3b** is shown. The other position can be found in Figure S3d in SI.

moieties around the alkene bond and is often encountered in stilbene molecular structures.[40] Unfortunately, it crystallized with two guest DMSO molecules, with 30 % of the crystal volume accessible to guests. An extended hydrogen-bonded network was not found in the crystal structure of compound NMe_2/F_5Ph **3b**. The molecules rather hydrogen bond with DMSO molecules (Figure 2a), arguably because the bulky dimethylamino headgroup hinders the formation of strong hydrogen bonds. For instance, it has been shown that a smaller headgroup, OMe, allows the formation of H-bonds between the NH linkers and the nitrogen atoms of the triazine in the crystalline structure of an analogous molecular glass.[41] An attempt was made to eliminate these residual DMSO molecules in the single crystals of **3b** used for the crystallographic analysis by drying them under vacuum. Although the resulting crystals were not suitable for a single crystal structure determination, IR spectra were recorded before and after the DMSO removal procedure (Figure S4a in SI). The spectrum of the crystalline **3b** containing DMSO molecules does not show any clear "free" NH band, which is consistent with the crystal structure of Figure 2a where both NH groups from the linkers are H-bonded to DMSO. Removal of DMSO under vacuum yields a spectrum with a strong and narrow "free" NH band very similar to that of the crystalline sample obtained by cooling the melt. These results lead to the conclusion that, despite the presence of DMSO molecules, almost identical interactions are found in the single crystal and in the crystals obtained by cooling, insuring that the comparisons made between the crystals of the two fluorinated compounds NHMe/F_5Ph **3a** and NMe_2/F_5Ph **3b** are reliable.

Compound NHMe/F_5Ph **3a** also crystallized in the triclinic space group P-1 with two molecules per unit cell. The conformation of individual molecules is similar to that for NMe_2/F_5Ph **3b** (Figure 2b, additional views can be found in Figure S5), with the methyl group of the NHMe headgroup oriented towards the stilbene group, thereby exposing the other face of the triazine ring to facilitate hydrogen bonding with neighboring molecules. Unlike analogue **3b**, no disorder was observed for the stilbene moieties. This absence of orientational disorder in the stilbene molecular structure could be explained by the presence of H-bonds creating a higher energy barrier for the pedal motion which hinders the conformational interconversion.[40] Compound NHMe/F_5Ph **3a** crystallized in a close-packed structure with no space accessible for guest molecules, with a Kitaigorodskii packing index of 71.4 % (calculated using the CALC VOID routine of PLATON),[42] which is significantly higher than the "usual" value for small organic molecules (65 %).[43] In contrast, previously published values for related mexylaminotriazine derivatives ranged from 60 to 65 %.[41] Unlike NMe_2/F_5Ph **3b**, molecules of compound NHMe/F_5Ph **3a** form H-bonded dimers between the NHMe headgroups and the triazine rings as shown in Figure 2b, where the stilbene and linker NH groups are not involved at all in the H-bonded pattern.

While 2,3,4,5,6-pentafluorostilbene (abbreviated as F_5-stilbene from hereon) is known to crystallize in extended π-stacked columns with alternating phenyl and pentafluophenyl groups (Figure S6), the crystal structures of compounds NHMe/F_5Ph **3a** and NMe_2/F_5Ph **3b** show a wholly different motif of aromatic interactions between the pentafluorostilbene moieties. Instead, **3a** and **3b** molecules form discrete dimers through extended π-π stacking where the mexyl ring and the stilbene alkene, which are both electron-rich, interact with the electron-deficient pentafluorophenyl and triazine rings, respectively (Figure 2c-d). For compound **3a**, closest centroid-centroid distances of 3.73 and 3.60 Å were observed with shift distances of 1.54 and 1.25 Å, respectively. For compound **3b**, slightly longer distances of 3.88 and 3.89 Å with shift distances of 1.67 and 1.81 Å were observed, likely a consequence of the more hindered dimethylamino headgroup.

A comparison of the IR spectra of the single crystal and amorphous states of compounds NHMe/F_5Ph **3a** and NMe_2/F_5Ph **3b** reveals differences in the intermolecular interactions present. Figure 3a shows for both compounds in the amorphous state (solid lines) a broad "bonded" NH band that is larger than the "free" band, whereas the "free" band is more intense in the crystalline state (dotted lines). This result validates that the NH of the linker groups of compounds **3a-b** partially H-bond in the amorphous state, although they do not in the crystalline structure (Figure 2) and thus impede the crystallization process. In both cases, the "free" NH bands in the crystalline state are narrower than in the amorphous state, indicating that the molecular environment of the "free" NH is much more specific in the crystalline state than in the amorphous sample presenting an inhomogeneous distribution of molecular environments and interaction strengths. It should be noted that the presence of two "free" NH bands for NHMe/F_5Ph **3a** may be due to the splitting of degenerated modes or intermolecularly coupled modes often encountered in vibrational spectra of crystals.[44]

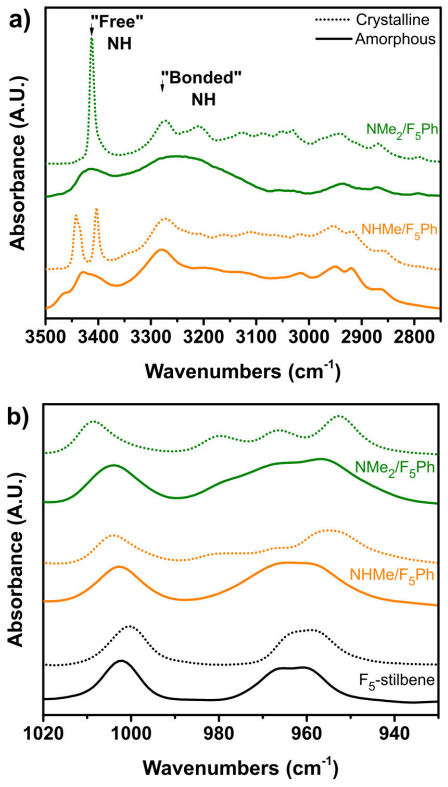

Figure 3. IR spectra showing a) the NH stretching region and b) the CF stretching region of compounds NHMe/F_5Ph **3a** (orange) and NMe_2/F_5Ph **3b** (green) in their crystalline (dotted line) and non-crystalline (solid line) states. The spectra of 2,3,4,5,6-pentafluorostilbene in the crystalline state and in solution (benzene-d_6) are also shown (black) for the CF stretching region.

The CF stretching regions, which can provide information on the aromatic interactions present,[45] also show differences between the crystalline and amorphous states, and also with the spectra of F_5-stilbene itself (Figure 3b). The spectra of the crystalline (dotted lines) compounds **3a** and **3b** both show a series of three bands at 980, 966 and 953 cm^{-1} (these bands are also retrieved in single crystals of NMe_2/F_5Ph **3b** after the DMSO removal procedure, see Figure S4b in SI), consistent with their similar π-stacking pattern in Figure 2c-d. This band pattern is not found in the single crystals of F_5-stilbene, which only presents a band with a maximum at 960 cm^{-1} and crystallizes with a different π-stacking pattern (Figure S6). Interestingly, the spectra observed in the non-crystalline state (solid lines) of F_5-stilbene and NHMe/F_5Ph **3a** are similar, featuring a band at 1002 cm^{-1} and a band with components at 966 and 960 cm^{-1}, evidencing that the molecular environment of the fluorinated ring is similar for these compounds. The spectrum of the amorphous NMe_2/F_5Ph **3b** also shows a band at 1002 cm^{-1} but, in contrast with the other compounds, it contains a lower wavenumber band with three components that corresponds to that observed in the crystalline state (it is broader in the amorphous sample because of the lack of long-range order). This result clearly reveals that the molecular environment of the pentafluorophenyl ring is already perturbed by aromatic interactions even if crystallization was prevented by the competing H-bonding interactions of the NH linkers, as observed in Figure 3a. The presence of these three band components in the amorphous sample indicates that π-π stacking interactions are more efficient in compound **3b** than in compound **3a** and explains the difference in their critical cooling rate. This result makes sense since in the headgroup of compound **3b**, the H is substituted by an additional methyl group. With the loss of a H-bond donor coupled with the additional steric bulk of the methyl group, compound **3b** is less efficient to establish H-bonds that kinetically impede the formation of π stacks in the viscous state above T_g. The π-π stacking can thus form and create a molecular environment analogous to that found in the crystalline structure, therefore driving crystallization and explaining the fast critical cooling rate needed to obtain compound **3b** in its glassy state. By opposition, compound **3a**, whose NHMe headgroup efficiently H-bonds and hinders the formation of π stacks, readily forms glasses upon slow cooling.

Competition of the Interactions

In order to rationalize the observed stacking of the pentafluorostilbene moieties and the H-bonded interactions in the crystalline structures, the geometries of an individual molecule of compound **2a-b** and **3a-b** were optimized using DFT calculations (B3LYP/6-311G(d,p)). One possible explanation emerges by looking at the coefficients of the HOMO (Figure 4a) and LUMO (Figure 4b) frontier orbitals of compound NHMe/F_5Ph **3a** (the HOMO and LUMO orbitals of compound **3b** are identical to those of compound **3a** and are shown in Figure S7a in SI). The HOMO orbital is mostly located on the electron-rich mexyl group, while the LUMO is located on the stilbene moiety, in contrast to non-fluorinated derivatives NHMe/Ph **2a** and NMe_2/Ph **2b**, where both the HOMO and LUMO are located on the stilbene moiety (Figure S7b-c in SI). In the π-π stacked dimer shown above in Figure 2d, the respective HOMO and LUMO orbitals of each molecules thus show

significant overlay. This specific packing geometry thus seems to arise at least partly from the interaction between frontier orbitals, in addition to the electrostatic interactions between electron-rich and electron-poor moieties.

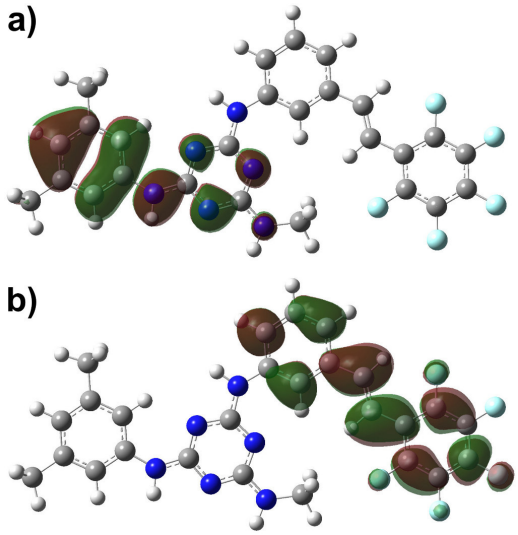

Figure 4. View of the frontier orbitals of compound NHMe/F_5Ph **3a** calculated by DFT (B3LYP/6-311G(d,p)) with the Gaussian 09 software. a) HOMO orbital, and b) LUMO orbital.

The relative propensities of the compounds studied to crystallize and the IR data suggest that the π-π stacking interaction formed by compounds **3a-b**, while different from the one in F_5-stilbene, is the driving force for the crystallization and for the crystalline packing of these derivatives. The H-bonding enthalpy measured experimentally[22] for the NHMe/F_5Ph **3a** compound in the viscous state using IR spectroscopy is -39 kJ/mol per molecule (an identical value was determined for compound NHMe/Ph **2a**), which corresponds to -13 kJ/mol for each individual H bond. Despite the fact that the π-π stacking arrangement for the dimers in Figure 2c-d is different from the classical aryl-perfluoroaryl interaction, it can be noted that these H-bond interaction values are comparable to the association energy reported between benzene and hexafluorobenzene in its sandwich complex form which is -20 kJ/mol.[47] Both types of non-covalent interactions therefore seem able to compete in the viscous state, with π-π stacking promoting crystallization (by limiting conformational flexibility) and the hydrogen bonding frustrating crystallization (by promoting the formation of different conformers), which is in agreement with previous studies.[29, 48] Indeed, in this family of compounds,[22] the primary factor responsible for impeding crystallization was revealed to be the presence of multiple conformers with similar energies and high interconversion barriers, and hydrogen bonding was shown to contribute as a kinetic trap by providing additional cohesion between molecules in both the viscous and vitreous states.[22-23]

Both types of interactions are moderately strong and are both likely to form reversibly above T_g. Moreover, both interactions are weaker than the energy barrier for the rotation of the NHR groups around the triazine ring.[22, 49-50] It is therefore unlikely that the relative strengths of these two particular types of interactions account for their impact on crystallization kinetics. A more likely explanation would thus involve the shape of the aggregates and their respective ability to pack efficiently. Indeed, for the molecules of compounds **3a-b** to crystallize from the viscous state, two barriers must be overcome: 1) as there is a higher density of hydrogen bonds in the amorphous phase than in the crystal, any superfluous hydrogen bonds must be broken during crystallization (an enthalpic barrier), and 2) the molecules must adopt the required conformation for π-π stacking (an entropic barrier). As the molecules involved in the π-π stacking interact in an extended face-to-face fashion, stricter conformational constraints are imposed on the molecules and a higher portion of the van der Waals surface of each molecule (52.0 Å² per molecule, 10.6 %, as determined from the crystal structure) is involved in the interaction. These constraints in turn lead to a more rigid structure, less conformational freedom, closer packing, and both less available space for forming secondary weak interactions with other neighboring molecules, and less variety of such interactions. In contrast, the molecules hydrogen bond in a lateral fashion, therefore the portion of the surface shared by the two molecules is minimal (9.4 Å² per molecule, 1.9 %). While the hydrogen-bonded dimer in the crystal structure is planar, molecules that hydrogen bond in the amorphous state are more likely to be twisted, and it is also possible that molecules form a single hydrogen bond with a neighbor rather than a pair as shown in Figure 2b, therefore decreasing even more the shared van der Waals surface. This leaves more surface available for interacting with other molecules through interactions that are less directional and more ambiguous, providing more conformational degrees of liberty and decreasing the probability that both molecules will exist in the same conformation, and giving rise to aggregates with awkward shapes that cannot pack in an optimal fashion.

Because non-fluorinated derivatives NHMe/Ph **2a** and NMe_2/Ph **2b** could not be crystallized, it is impossible to clearly determine how the stilbene moieties would interact in the crystalline state. Stilbene itself crystallizes in a zipper-like pattern, with each molecule forming two types of edge-to-face π-π stacking interactions with four neighboring molecules.[40] Unlike the face-to-face π-π stacking involving the pentafluorinated rings, these interactions are much weaker individually. Furthermore, in each of these interactions, an average of 2.4 Å² of the van der Waals surface per molecule is shared (1.1 % of the total surface), which is significantly lower than for the extended π-π stacking interaction of compounds **3a-b** or that of F_5-stilbene itself (20.6 Å² per molecule, 8.0 %). As a result, the stilbene moieties are expected to interact in a less directional and homogeneous fashion, and not to compete significantly with the stronger hydrogen bonds. This would explain why compounds **2a-b** completely failed to crystallize.

Conclusion

Herein, the impact of the interplay between two types of intermolecular interactions, hydrogen bonding and π-π stacking, on crystallization and glass-forming ability was

studied by comparing two pairs of mexylaminotriazine derivatives containing 2,3,4,5,6-pentafluorostilbene moieties, a supramolecular synthon known for forming face-to-face π-π stacking, with their non-fluorinated analogues. Each pair included one derivative containing an easily accessible H-bond donor group and one derivative without it. While all four compounds studied showed the ability to form glasses, both pentafluorostilbene derivatives showed crystallization with varying crystallization kinetics, whereas the non-fluorinated derivatives could not be successfully crystallized. The crystal structures of both pentafluorostilbene analogues were determined by X-ray crystallography and showed an extended π-π stacking interaction involving all four aromatic rings (different from the stacking observed in 2,3,4,5,6-pentafluorostilbene) and less hydrogen bonding than in the amorphous state. Hydrogen bonding and π-π stacking thus act in competition in the amorphous material, with π-π stacking promoting crystallization and hydrogen bonding impeding it. It is concluded that this behavior is due to the constraints imposed on the molecules by the interactions: π-π stacking interactions involve a significant fraction of the van der Waals surface of the molecules and require the molecules to adopt a specific conformation, whereas hydrogen bonds form laterally and involve a small portion of the surface, thereby offering more conformational freedom to the molecules and allowing a higher variety of secondary interactions. This study also highlights the effect of substituent groups on balancing the relative importance of available interactions. In the present case, substituting a NH for a NMe group simultaneously decreased the formation of H bonds by providing one less H-bond donor and increasing steric bulk, resulting instead in the formation of a competing π-π stacking interaction, even in the amorphous state. These findings provide valuable insights for both the crystal and glass engineering of molecular materials.

Experimental Section

General. 2-Methylamino-4-mexylamino-6-[(3-formylphenyl)amino]-1,3,5-triazine (**1a**),[19] 2-dimethylamino-4-phenylamino-6-dichloro-1,3,5-triazine,[51] and 2,3,4,5,6-pentafluorobenzyltriphenylphosphonium bromide[39] were prepared according to literature procedures. All other reagents and solvents were purchased from commercial sources and used without further purification. All reactions were performed under ambient atmosphere. SiliaFlash P60 grade silica gel and TLC plates were purchased from SiliCycle. ^{1}H NMR spectra were recorded on a Bruker Avance 400 MHz or a Varian Mercury 300 MHz spectrometer at 298 K or 363 K (as indicated). ^{13}C NMR spectra were recorded on a Varian Mercury 300 MHz spectrometer at 298 K. ^{19}F NMR spectra were recorded on a Bruker Avance 400 MHz spectrometer at 298 K. Decomposition analyses of molecular glasses were obtained using a TGA 2950 thermogravimetric analyzer (TA Instruments) at a heating rate of 10 °C/min under a nitrogen atmosphere. Transition temperatures (glass transition temperature T_g, crystallization temperature T_c and melting temperature T_m) were recorded by DSC with a PerkinElmer DSC 8500 calorimeter calibrated with indium using a heating rate of 10 °C/min. T_g were reported after an initial cycle of heating and a ballistic cooling, and as the average of the values observed in heating. Critical cooling rates (R_c) were determined by cooling the melted compounds at different rates, from fast (100 °C/min) to slow (0.05 °C/min) until the compounds showed any sign of crystallization (either crystallization exotherm upon cooling or a residual enthalpy of melting upon heating in cases where cold crystallization followed by melting was observed). IR spectra were recorded on a Tensor 27 FT-IR spectrometer (Bruker Optics) equipped with a liquid nitrogen-cooled HgCdTe detector. For ambient temperature measurements, films (unless otherwise noted) were directly cast from CH_2Cl_2 solutions on the silicon crystal of a MIRacle (Pike Technologies) attenuated total reflection (ATR) accessory. The spectrum of crystalline F_5-stilbene was recorded using a VariGATR (Harrick Scientific) accessory. For variable-temperature spectroscopy, a Golden Gate (Specac) diamond ATR accessory was used. Samples were directly deposited on the ATR crystal, then heated to 200 °C, followed by a 3 min isotherm before being cooled down using a rate of 2 °C/min. Single beam spectra were recorded at each 5 °C by averaging 100 scans with a 4 cm^{-1} resolution. Background spectra were recorded for each temperature. The average number of H-bonded NH groups per molecule and the total enthalpy of H-bond formation were computed from the variable-temperature spectra recorded above T_g using a principal component analysis and SMMA procedure as previously reported by Laventure et al.[22]The geometries of compound **2a-b** and **3a-b** were optimized and their HOMO and LUMO orbitals were calculated using the Gaussian 09 software with the B3LYP functional and the 6-311G(d,p) basis set.

2-Dimethylamino-4-phenylamino-6-[(3-formylphenyl)amino]-1,3,5-triazine (1b). A solution of 2-dimethylamino-4-phenylamino-6-dichloro-1,3,5-triazine (3.41 g, 13.7 mmol) and 3-aminobenzaldehdye diethylacetal (3.47 g, 17.8 mmol) in THF (50 mL) in a round-bottomed flask equipped with a magnetic stirrer and a water-jacketed condenser was refluxed for 18 h, at which point 1M aqueous HCl (20 mL) was added and the reflux was continued an additional 1h. Ethyl ether and H_2O were added, causing a precipitate to form. The precipitate was collected by filtration, washed with H_2O and ethyl ether, then the crude product was recrystallized from hot toluene to give 1.55 g pure compound **1b** (4.64 mmol, 34 %). T_g 51 °C, T_m 178 °C; FT-IR (ATR/CH_2Cl_2) 3404, 3286, 3201, 3109, 3057, 2931, 2868, 1693, 1617, 1582, 1547, 1525, 1509, 1496, 1483, 1434, 1418, 1403, 1367, 1318, 1305, 1265, 1231, 1175, 1087, 1062, 996, 976, 897, 805, 787, 753, 735, 691 cm^{-1}; ^{1}H NMR (300 MHz, DMSO-d_6, 298 K) δ 9.95 (s, 1H), 9.41 (br s, 1H), 9.13 (br s, 1H), 8.45 (s, 1H), 8.02 (br s, 1H), 7.77 (d, ^{3}J = 8.2 Hz, 2H), 7.48 (d, ^{3}J = 5.3 Hz, 2H), 7.25 (t, ^{3}J = 7.6 Hz, 2H), 6.94 (t, ^{3}J = 7.6 Hz, 1H), 3.14 (s, 6H) ppm; ^{13}C NMR (75 MHz, DMSO-d_6) δ 193.5, 165.6, 164.3, 141.7, 140.6, 137.0, 129.6, 128.8, 125.9, 123.3, 122.1, 120.5, 120.3, 36.4 ppm; HRMS (ESI, MNa^+) calcd. for $C_{18}H_{18}NaN_6O$ *m/e*: 357.1434, found: 357.1446.

3-(2-Methylamino-4-mexylamino-1,3,5-triazin-6-yl)aminostilbene (2a). Benzyltriphenylphosphonium

chloride (0.428 g, 1.10 mmol) was dissolved in dry DMF (10 mL) under N_2 atmosphere in a dry round-bottomed flask equipped with a magnetic stirrer. NaH (60 wt% in mineral oil, 0.048 g, 1.20 mmol) was added, and the mixture was stirred 45 min at ambient temperature. 2-Methylamino-4-mexylamino-6-[(3-formylphenyl)amino]-1,3,5-triazine **1** (0.458 g, 1.00 mmol) was added, and the mixture was stirred for 18 h at 60 °C under N_2 atmosphere, after which the mixture was poured into H_2O and stirred 5 minutes at ambient temperature. The resulting precipitate was collected by filtration, washed with H_2O and redissolved in CH_2Cl_2. The solution was dried over Na_2SO_4, filtered, and the volatiles were evaporated under reduced pressure. Chromatography on silica using AcOEt/hexanes 1:1 as eluent yielded 0.286 g compound **2a** as a 3:1 mixture of *E*/*Z* isomers that could not be satisfactorily separated (0.677 mmol, 68 %). T_g (*E*/*Z*) 78 °C; FT-IR (ATR/CH_2Cl_2) 3411, 3279, 3191, 3081, 3057, 3024, 2973, 2947, 2917, 2866, 1578, 1557, 1513, 1427, 1398, 1360, 1323, 1301, 1241, 1211, 1185, 1167, 1085, 1030, 998, 960, 883, 841, 809, 782, 748, 693 cm^{-1}; ^1H NMR (*E*, 400 MHz, DMSO-d_6, 363 K) δ 8.71 (br s, 1H), 8.53 (br s, 1H), 8.03 (s, 1H), 7.69 (d, ^3J = 7.6 Hz, 1H), 7.40 (s, 2H), 7.26 (m, 3H), 7.21 (d, ^3J = 7.8 Hz, 2H), 7.15 (s, 2H), 6.62 (s, 1H), 6.61 (d, ^3J = 7.1 Hz, 1H), 2.93 (d, ^3J = 4.5 Hz, 3H), 2.25 (s, 6H) ppm; ^1H NMR (*Z*, 400 MHz, DMSO-d_6, 363 K) δ 8.62 (br s, 1H), 8.43 (br s, 1H), 7.71 (d, ^3J = 7.8 Hz, 1H), 7.64 (s, 1H), 7.39 (s, 2H), 7.26 (m, 3H), 7.21 (d, ^3J = 7.8 Hz, 2H), 7.15 (s, 2H), 6.82 (d, ^3J = 7.3 Hz, 1H), 6.62 (s, 1H), 6.62 (s, 1H), 6.51 (br s, 1H), 2.87 (d, ^3J = 4.3 Hz, 3H), 2.25 (s, 6H) ppm; ^{13}C NMR (75 MHz, $CDCl_3$) δ 166.7, 164.3, 139.5, 138.6, 138.3, 137.9, 137.3, 130.3, 130.1, 128.8, 128.8, 128.6, 128.1, 127.6, 127.1, 126.5, 124.9, 123.2, 121.2, 120.4, 119.4, 119.0, 118.4, 27.7, 21.4 ppm; HRMS (ESI, MNa^+) calcd. for $C_{26}H_{26}NaN_6$ *m*/*e*: 445.2111, found: 445.2123.

Crystal Structure Determination. Crystals of compound NHMe/F_5Ph **3a** were prepared by annealing the melted compound at 150 °C for 24 h and single crystals of **3b** were crystallized from DMSO/CH_2Cl_2. For each compound, a suitable crystal was selected and mounted on a cryoloop on a Bruker Venture Metaljet diffractometer. The crystal was kept at 100 K (**3a**) and 110 K (**3b**) during data collection. Using Olex2,[52] the structure was solved with the XT[53] structure solution program using Intrinsic Phasing and refined with the XL[54] refinement package using Least Squares minimization. In the case of **3b**, the crystal was a two-components twins with refined fraction of 0.9567(7) and 0.0433(7).

Crystal Data. Compound NHMe/F_5Ph **3a** $C_{26}H_{21}F_5N_6$ (M =512.49 g/mol): triclinic, space group P-1 (no. 2), *a* = 8.0372(7) Å, *b* = 9.8143(8) Å, *c* = 14.9100(12) Å, *α* = 87.061(5)°, *β* = 76.319(5)°, *γ* = 84.542(5)°, V = 1137.04(17) Å^3, Z = 2, T = 100 K, μ(GaKα) = 0.662 mm^{-1}, D_{calc} = 1.497 g/cm^3, 37272 reflections measured (5.31° ≤ 2Θ ≤ 121.608°), 5245 unique (R_{int} = 0.0635, R_{sigma} = 0.0372) which were used in all calculations. The final R_1 was 0.0550 (I > 2σ(I)) and wR_2 was 0.1614 (all data).

Compound NMe_2/F_5Ph **3b** $C_{29}H_{31}F_5N_6O_2S_2$ (M =654.72 g/mol): triclinic, space group P-1 (no. 2), *a* = 7.9866(3) Å, *b* = 11.0761(4) Å, *c* = 17.2150(6) Å, *α* = 90.6702(17)°, *β* = 99.6908(17)°, *γ* = 99.0590(17)°, V = 1481.25(9) Å^3, Z = 2, T = 110 K, μ(GaKα) = 1.461 mm^{-1}, D_{calc} = 1.468 g/cm3, 6736 reflections measured (4.534° ≤ 2Θ ≤ 121.306°), 6736 unique (R_{int} = 0.0412, R_{sigma} = 0.0352) which were used in all calculations. The final R_1 was 0.0563 (I > 2σ(I)) and wR_2 was 0.1537 (all data).

ASSOCIATED CONTENT

Supporting Information. Synthesis of compounds **2b** and **3a**-**b**, representative DSC scans, variable-temperature IR spectra of compound NMe_2/F_5Ph **3b**, additional views of crystalline structures of NMe_2/F_5Ph **3b** and NHMe/F_5Ph **3a**, IR spectra of NMe_2/F_5Ph **3b** crystals before and after the DMSO removal attempt, HOMO and LUMO orbitals for compounds **2a-b** and **3b**, and NMR spectra. This material is available free of charge via the Internet at http://pubs.acs.org.

AUTHOR INFORMATION

Corresponding Author

*Author to whom correspondence should be addressed: olivier.lebel@rmc.ca

Author Contributions

The manuscript was written through contributions of all authors. All authors have given approval to the final version of the manuscript.

Funding Sources

This research was funded by the Fonds de Recherche du Québec – Nature et Technologies (FRQNT #2012-PR-147034), the Natural Sciences and Engineering Research Council of Canada (NSERC #312493), and the Canadian Defence Academy Research Programme (CDARP) from RMC.

Notes

Marvin was used for drawing, displaying and characterizing chemical structures, substructures and reactions, Marvin 15.1.12, 2015, ChemAxon (http://www.chemaxon.com).

ACKNOWLEDGMENT

AL thanks the Natural Sciences and Engineering Research Council (NSERC) of Canada for a Vanier graduate scholarship. The authors are also grateful to Dr. René Gagnon (Université de Sherbrooke) for mass spectrometry analysis, and to WestGrid and Compute Canada for access to the supercomputer Grex for the DFT calculations.

REFERENCES

1. Angell, C. A., *Science* **1995,** *267*, 1924-1935.
2. Ediger, M. D.; Angell, C. A.; Nagel, S. R., *J. Phys. Chem.* **1996,** *100*, 13200-13212.
3. Berthier, L.; Ediger, M. D., *Phys. Today* **2016,** *69*, 40-46.
4. Shirota, Y., *J. Mater. Chem.* **2000,** *10*, 1-25.
5. Shirota, Y., *J. Mater. Chem.* **2005,** *15*, 75-93.
6. Shirota, Y.; Kageyama, H., *Chem. Rev.* **2007,** *107*, 953-1010.
7. Lygaitis, R.; Getautis, V.; Grazulevicius, J. V., *Chem. Soc. Rev.* **2008,** *37*, 770-788.
8. Ping, W.; Paraska, D.; Baker, R.; Harrowell, P.; Angell, C. A., *J. Phys. Chem. B* **2011,** *115*, 4696-4702.

9. Liu, T.; Cheng, K.; Salami-Ranjbaran, E.; Gao, F.; Glor, E. C.; Li, M.; Walsh, P. J.; Fakhraai, Z., *Soft Matter* **2015,** *11*, 7558-7566.
10. Ishow, E.; Lebon, B.; He, Y.; Wang, X.; Bouteiller, L.; Galmiche, L.; Nakatani, K., *Chem. Mater.* **2006,** *18*, 1261-1267.
11. Nakano, H.; Takahashi, T.; Kadota, T.; Shirota, Y., *Adv. Mater.* **2002,** *14*, 1157-1160.
12. Traskovskis, K.; Mihailovs, I.; Tokmakovs, A.; Jurgis, A.; Kokars, V.; Rutkis, M., *J. Mater. Chem.* **2012,** *22*, 11268-11276.
13. Yoshiiwa, M.; Kageyama, H.; Shirota, Y.; Wakaya, F.; Gamo, K.; Takai, M., *Appl. Phys. Lett.* **1996,** *69*, 2605-2607.
14. Toshiaki, K.; Hiroshi, K.; Fujio, W.; Kenji, G.; Yasuhiko, S., *Chem. Lett.* **2004,** *33*, 706-707.
15. Yu, L., *Adv. Drug. Deliv. Rev.* **2001,** *48*, 27-42.
16. Gao, P., *Mol. Pharm,* **2008,** *5*, 903-904.
17. Lebel, O.; Maris, T.; Perron, M.-È.; Demers, E.; Wuest, J. D., *J. Am. Chem. Soc.* **2006,** *128*, 10372-10373.
18. Wuest, J. D.; Lebel, O., *Tetrahedron* **2009,** *65*, 7393-7402.
19. Eren, R. N.; Plante, A.; Meunier, A.; Laventure, A.; Huang, Y.; Briard, J. G.; Creber, K. J.; Pellerin, C.; Soldera, A.; Lebel, O., *Tetrahedron* **2012,** *68*, 10130-10144.
20. Laventure, A.; Soldera, A.; Pellerin, C.; Lebel, O., *New J. Chem.* **2013,** *37*, 3881-3889.
21. Damasceno, P. F.; Engel, M.; Glotzer, S. C., *Science* **2012,** *337*, 453-457.
22. Laventure, A.; De Grandpré, G.; Soldera, A.; Lebel, O.; Pellerin, C., *Phys. Chem. Chem. Phys.* **2016,** *18*, 1681-1692.
23. Plante, A.; Mauran, D.; Carvalho, S. P.; Pagé, J. Y. S. D.; Pellerin, C.; Lebel, O., *J. Phys. Chem. B* **2009,** *113*, 14884-14891.
24. Martinez, C. R.; Iverson, B. L., *Chem. Sci.* **2012,** *3*, 2191-2201.
25. Wheeler, S. E.; Bloom, J. W. G., *J. Phys. Chem. A* **2014,** *118*, 6133-6147.
26. Mignon, P.; Loverix, S.; Steyaert, J.; Geerlings, P., *Nucleic Acids Res.* **2005,** *33*, 1779-1789.
27. Saenger, W., Forces Stabilizing Associations Between Bases: Hydrogen Bonding and Base Stacking. In *Principles of Nucleic Acid Structure*, Springer New York: New York, NY, 1984; pp 116-158.
28. Berl, V.; Huc, I.; Khoury, R. G.; Krische, M. J.; Lehn, J.-M., *Nature* **2000,** *407*, 720-723.
29. Aytun, T.; Barreda, L.; Ruiz-Carretero, A.; Lehrman, J. A.; Stupp, S. I., *Chem. Mater.* **2015,** *27*, 1201-1209.
30. Yuan, M. S.; Wang, D. E.; Xue, P.; Wang, W.; Wang, J. C.; Tu, Q.; Liu, Z.; Liu, Y.; Zhang, Y.; Wang, J., *Chem. Mater.* **2014,** *26*, 2467-2477.
31. Patrick, C. R.; Prosser, G. S., *Nature* **1960,** *187*, 1021-1021.
32. Coates, G. W.; Dunn, A. R.; Henling, L. M.; Ziller, J. W.; Lobkovsky, E. B.; Grubbs, R. H., *J. Am. Chem. Soc.* **1998,** *120*, 3641-3649.
33. Reichenbacher, K.; Suss, H. I.; Hulliger, J., *Chem. Soc. Rev.* **2005,** *34*, 22-30.
34. Hsu, S.-M.; Lin, Y.-C.; Chang, J.-W.; Liu, Y.-H.; Lin, H.-C., *Angew. Chem. Int. Ed.* **2014,** *53*, 1921-1927.
35. Weck, M.; Dunn, A. R.; Matsumoto, K.; Coates, G. W.; Lobkovsky, E. B.; Grubbs, R. H., *Angew. Chem. Int. Ed.* **1999,** *38*, 2741-2745.
36. Gray, T.; Kim, T. D.; Knorr, D. B.; Luo, J. D.; Jen, A. K. Y.; Overney, R. M., *Nano Lett.* **2008,** *8*, 754-759.
37. Kim, T.-D.; Kang, J.-W.; Luo, J.; Jang, S.-H.; Ka, J.-W.; Tucker, N.; Benedict, J. B.; Dalton, L. R.; Gray, T.; Overney, R. M.; Park, D. H.; Herman, W. N.; Jen, A. K. Y., *J. Am. Chem. Soc.* **2007,** *129*, 488-489.
38. Zhou, X. H.; Luo, J. D.; Huang, S.; Kim, T. D.; Shi, Z. W.; Cheng, Y. J.; Jang, S. H.; Knorr, D. B.; Overney, R. M.; Jen, A. K. Y., *Adv. Mater.* **2009,** *21*, 1976-1981.
39. Clément, S.; Meyer, F.; De Winter, J.; Coulembier, O.; Vande Velde, C. M. L.; Zeller, M.; Gerbaux, P.; Balandier, J.-Y.; Sergeyev, S.; Lazzaroni, R.; Geerts, Y.; Dubois, P., *J. Org. Chem.* **2010,** *75*, 1561-1568.
40. Harada, J.; Ogawa, K., *J. Am. Chem. Soc.* **2001,** *123*, 10884-10888.
41. Wang, R.; Pellerin, C.; Lebel, O., *J. Mater. Chem.* **2009,** *19*, 2747-2753.
42. Spek, A., *J. Appl. Crystallogr.* **2003,** *36*, 7-13.
43. Kitaigorodskii, A. I., *Molecular Crystals and Molecules*. Academic Press: New York, 1973.
44. Chalmers, J. M., Mid-Infrared Spectroscopy of the Condensed Phase. In *Handbook of Vibrational Spectroscopy*, Chalmers, J. M.; Griffiths, P. R., Eds. John Wiley & Sons, Ltd: Chichester, 2002; Vol. 1, p 128.
45. Meić, Z.; Güsten, H., *Spectrochim. Acta, Part A* **1980,** *36*, 1021-1027.
46. The 6-31G(d,p) basis set was used for this calculation because the 6-311G(d,p) basis set gave a geometry inconsistent with the crystal structure.
47. Tsuzuki, S.; Uchimaru, T.; Mikami, M., *J. Phys. Chem. A* **2006,** *110*, 2027-2033.
48. Seth, S. K.; Sarkar, D.; Kar, T., *CrystEngComm* **2011,** *13*, 4528-4535.
49. Hyengoyan, A. P.; Mamyan, S. S.; Gomktsyan, T. A.; Hambardzumyan, E. N.; Vorskanyan, A. S.; Eliazyan, K. A.; Pivazyan, V. A.; Dovlatyan, V. V., *Chem. Heterocycl. Compd.* **2005,** *41*, 1059-1061.
50. Plante, A.; Palato, S.; Lebel, O.; Soldera, A., *J. Mater. Chem. C* **2013,** *1*, 1037-1042.
51. Eaton, D. C. L., Boris N. DE2051521, 1971.
52. Dolomanov, O. V.; Bourhis, L. J.; Gildea, R. J.; Howard, J. A. K.; Puschmann, H., *J. Appl. Crystallogr.* **2009,** *42*, 339-341.
53. Sheldrick, G., *Acta Crystallogr. Sect. C: Cryst. Struct. Commun.* **2015,** *71*, 3-8.
54. Sheldrick, G., *Acta Crystallogr. Sect. A: Found. Crystallogr.* **2008,** *64*, 112-122.

SYNOPSIS TOC

We studied the impact of competing non-covalent interactions, H-bonds and strong π-π stacking, on the crystallization or vitrification of mexylaminotriazine derivatives incorporating stilbene or pentafluorostilbene groups. X-ray

diffraction, infrared spectroscopy and DFT calculations reveal that H-bonds favor glass formation while π-π stacking promotes crystallization by imposing higher conformational constraint. This work shows how molecular design enables tipping crystal or glass formation by balancing competing intermolecular interactions.